Relationship between Material Properties and Transparent Heater Performance for Both Bulk-like and Percolative Nanostructured Networks

Sophie Sorel,[†] Daniel Bellet,[‡] and Jonathan N Coleman[†,*]

[†]School of Physics, CRANN and AMBER, Trinity College Dublin, Dublin 2, Ireland and [‡]Laboratoire des Matériaux et du Génie Physique, 3 Parvis Louis Néel, CS 50257, CNRS, Grenoble INP, 38 016 Grenoble, France

ABSTRACT Transparent heaters are important for many applications and in the future are likely to be fabricated from thin, conducting, nanostructured networks. However, the electrical properties of such networks are almost always controlled by percolative effects. The impact of percolation on heating effects has not been considered, and the material parameter combinations that lead to efficient performance are not known. In fact, figures of merit for transparent heaters have not been elucidated, either in bulk-like or percolative systems. Here, we develop a simple yet comprehensive model describing the operation of transparent heaters. By considering the balance of Joule heating *versus* power dissipated by both convection and radiation, we derive an expression for the time-dependent heater temperature as a function of both electrical and thermal parameters. This equation can be modified to describe the relationship between temperature, optical transmittance, and electrical/thermal parameters in both bulk-like and percolative systems. By performing experiments on silver nanowire networks, systems known to display both bulk-like and percolative regimes, we show the model to describe real systems extremely well. This work shows the performance of transparent heaters in the percolative regime to be significantly less efficient compared to the bulk-like regime, implying the diameter of the nanowires making up the network to be critical. The model allows the identification of figures of merit for networks in both bulk-like and percolative regimes. We show that metallic nanowire networks are most promising, closely followed by CVD graphene, with networks of solution-processed graphene and carbon nanotubes being much less efficient.

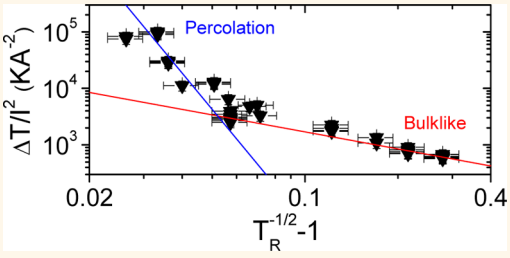

KEYWORDS: percolation · radiative · convective · thermal · graphene · nanotubes

The past few years have seen a considerable amount of research devoted to the study of nanostructured transparent conducting materials. The aim of this research is to use nanomaterials to replace traditional transparent conductors such as indium tin oxide (ITO).[1] While transparent conducting oxides have provided good service for many years,[2] they face a number of difficulties that make them unsuitable for next-generation applications. For example, the rising price of indium has made ITO increasingly expensive. In addition, all transparent metal oxides are brittle[3] and expensive to deposit over large areas. This makes them inappropriate for many future uses given the anticipated shift to large-area, flexible display technology.

A number of different nanomaterials have been extensively tested in this space. Probably the most studied are solution-processed networks of carbon nanotubes,[4−6] graphene nanosheets,[7,8] and metallic nanowires (NWs)[9−17] as well as vapor-grown graphene films.[18] These materials have been used as electrodes in a range of applications including light-emitting diodes, solar cells, and transparent capacitors.[19,20] However, more recently, attention has turned to using nanostructured transparent conductors as transparent heaters.[21−30] Transparent heaters are simply conducting films that are thin enough to be transparent but can be heated up on application of a voltage. For a given combination of electrical and thermal properties, the steady-state temperature increase is set by balance of

* Address correspondence to colemaj@tcd.ie.

Received for review February 4, 2014 and accepted April 2, 2014.

Published online April 02, 2014
10.1021/nn500692d

Joule heating and heat dissipation and can be controlled *via* the voltage. Such devices are important for a number of applications from defogging of windows or mirrors[21] to performance optimization of liquid crystalline displays *via* temperature control[31] to art conservation.[32]

One of the most commonly used, commercially available transparent heater materials is ITO. In fact, one of the earliest patents describing transparent, conducting doped tin oxide films explicitly described de-icing aircraft windscreens as a potential application.[33] However, ITO transparent heaters suffer the same problems that ITO faces in other transparent conducting applications, namely, cost, flexibility, and areal scaling. As with other transparent conducting applications, a number of researchers have turned to nanostructured materials, particularly carbon nanotubes,[23,24,26,28,29] graphene,[18,25,34] silver nanowires[22,27,30,35] and hybrid systems.[36,37] The results have been very promising with reported temperature increases of up to 140 K for 4 W input power.[29]

However, there is a considerable amount of work required before it becomes clear what the true capabilities of the various nanomaterials are. In addition, it is very difficult to compare the performance of the various materials studied. For example, no well-defined figure of merit (FoM) is generally reported to facilitate benchmarking and performance comparison. Part of the problem is the lack of a comprehensive theoretical framework to analyze transparent heater behavior. Only one paper discusses the power balance in any detail, driving an approximate relationship between temperature increase and time, current, voltage, and heat transfer parameters (radiative losses are neglected).[21] No papers discuss the relationship between temperature increase, current, voltage, and heat transfer parameters with transmittance, which we view as critically important. Theoretical understanding of such relationships not only would facilitate understanding of the heating mechanisms but would allow the definition of a FoM that would allow ranking of materials and selection of most promising materials for further study.

Here we address these problems by developing a comprehensive yet simple theoretical framework that describes the relationships between temperature increase, transparency, and both electrical and thermal properties. This framework can be applied to standard transparent heater materials such as ITO in a straightforward way by considering standard relationships between transmittance and sheet resistance. However, parallel experimental studies using networks of AgNWs show that such an approach can be applied only to nanostructured networks that are relatively thick. In thinner networks, connectivity effects become important, and the electrical properties become limited by percolation theory. Here we have developed an additional theoretical framework that is appropriate to the percolation regime. We show that experimental results for the steady-state temperature increase for AgNW networks of different transparencies clearly display two regimes, which are perfectly described by the normal (*i.e.*, bulk) and percolative theoretical frameworks. Access to theoretical models allows us to define FoMs appropriate to both normal and percolative transparent heaters. By analyzing literature results, we can show that AgNW networks, closely followed by CVD graphene films, are by far the best performing nanostructured transparent heaters.

RESULTS AND DISCUSSION

The aim of this work is to develop an understanding of the factors that limit the performance of transparent heaters. We will do this by developing a simple but comprehensive model describing the dependence of network temperature on current, voltage, sheet resistance, and transmittance in both the steady state and time-dependent regimes. This model will be applied to networks whose electrical properties are bulk-like and to those limited by percolative effects. We will test the validity of this model by comparison with experiments.

The model systems we will use in this work are networks of silver nanowires. These systems have been well studied by a range of authors and are reasonably well understood.[9,11−14,38−42] Before developing a mathematical model to describe transparent heaters, we will fully characterize the optoelectric properties of spray-deposited AgNW networks, allowing them to be used as an appropriate model system. We use spray-casting[14] to deposit AgNW networks of various thickness (*i.e.*, various nanowire densities) onto polyethylene terephthalate (PET) substrates (substrate thickness ∼135 μm). From the amount of AgNW deposited, we roughly estimate the nanowire densities to range from ∼10 to 150 mg/m^2, giving average thicknesses of ∼15 to 300 nm (assuming a porosity of ∼95%).[9] This procedure results in films of various transparencies that appear uniform to the naked eye. Examples of networks with transparencies, T_R, of 97% and 57% are shown in Figure 1A and B, respectively. Closer examination using SEM or He ion microscopy (Figure 1C−E) shows such networks to consist of arrays of nanowires that are randomly arranged in the plane of the network. We measured the transmittance and sheet resistance of a wide range of networks as shown in Figure 1F. The thickest networks had (R_s, T_R) combinations of (8.2 Ω/□, 57%). These values increased smoothly to (2 × 10^7 Ω/□, 98.5%) for the thinnest networks. As a benchmark, we note that the network with a transmittance of 90.5% had a sheet resistance of 53 Ω/□. This compares reasonably favorably to the literature for metal nanowire networks,[43] although a number of papers have reported lower sheet resistances for $T_R \approx 90\%$.[38] However, the results presented

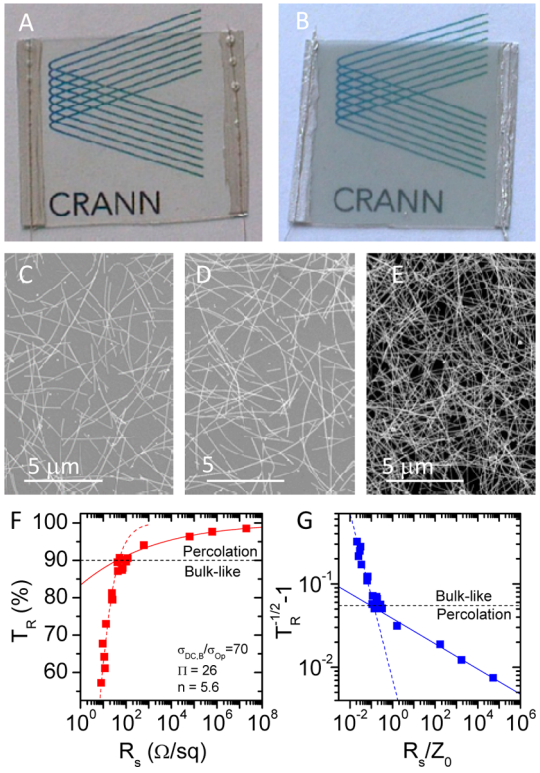

Figure 1. (A, B) Photographs of spray-coated AgNW networks with optical transmittance of (A) 97% and (B) 57%. (C, D) SEM images of AgNW networks with transmittance of (C) T_R = 94% and (D) T_R = 90%. (E) He ion micrograph of an AgNW network with T_R = 80%. (F) Optical transmittance (550 nm) plotted *versus* sheet resistance for all the networks prepared in this study. The red lines are fits to eq 1 (dashed) and eq 2 (solid). The fit constants are given in the panel. The black horizontal line indicates the boundary between bulk-like and percolative behavior. (G) The same data in F, plotted to illustrate linear behavior.

here are far superior to reported values for transparent conductors of almost all other nanomaterials.[43]

For thin conducting films, the optical transmittance (at a given wavelength) can be related to the sheet resistance, R_s, by[4,42,44]

$$T_R = \left(1+\frac{Z_0}{2R_s}\frac{\sigma_{Op}}{\sigma_{dc,B}}\right)^{-2} \quad (1)$$

where Z_0 is the impedance of free space (377 Ω). (We note that for films of nanostructured objects such as nanowires, this expression holds as long as the film thickness is >2.33D, where D is the nanowire diameter; see below.[42]) Here the ratio of bulk dc to optical conductivity, $\sigma_{dc,B}/\sigma_{Op}$, can be considered a figure of merit, with high values giving the desired properties (high T_R coupled with low R_s). It has been pointed out that eq 1 is not strictly applicable for many nanostructured films because it assumes the interaction of light solely with free carriers, which is not strictly true in the visible region.[45] However, this expression generally describes experimental data for relatively thick films rather well and has the advantage that values of $\sigma_{dc,B}/\sigma_{Op}$ are known for a range of nanostructured thin films.[43] In addition, because the optical conductivity in this expression can be shown to be proportional to the Lambert–Beer absorption coefficient, α,[42] we feel it is acceptable to use once $\sigma_{dc,B}/\sigma_{Op}$ is treated as a figure of merit rather than a physical property. It is worth noting that the entire analysis described below can be performed equally well using an expression that is analogous to eq 1 but is based on the Lambert–Beer law (*i.e.*, $T = e^{-\alpha/\sigma_{dc,B}R_s}$).[42]

We can test applicability of eq 1 to our data by plotting $T_R^{-1/2} - 1$ *versus* R_s/Z_0 (Figure 1G). Here a straight line on a log–log plot with slope of −1 is characteristic of bulk behavior. This is indeed the case, allowing us to obtain $\sigma_{dc,B}/\sigma_{Op}$ = 70 (using this value, we have plotted eq 1 as a dotted line on Figure 1G for comparison). This value is smaller than values reported for other metallic nanowire networks (83 < $\sigma_{dc,B}/\sigma_{Op}$ < 453; see a recent review for tabulated data[43]), probably due to source to source variations in the nanowires (or perhaps the organic stabilizing coating).

However, eq 1 fits the data only for networks with R_s/Z_0 < 0.12, with the data diverging for thinner networks. This is a relatively common phenomenon[9,46–48] and has been attributed to percolation effects.[42] For such thin networks, a new relationship between T_R and R_s has been proposed:[42]

$$T_R = \left[1+\frac{1}{\Pi}\left(\frac{Z_0}{R_s}\right)^{1/(n+1)}\right]^{-2} \quad (2)$$

where n is the percolation exponent and Π is known as the percolative figure of merit:

$$\Pi = 2\left[\frac{\sigma_{dc,B}/\sigma_{Op}}{(Z_0 t_{min}\sigma_{Op})^n}\right]^{1/(n+1)} \quad (3)$$

Here, t_{min} is the transition thickness, below which the dc conductivity becomes thickness dependent (*i.e.*, eq 2 applies for $t < t_{min}$, while eq 1 applied for $t > t_{min}$). Analysis of these equations shows that large values of Π coupled with low values of n are desirable to achieve low R_s and high T_R.[42] Furthermore, we showed empirically that networks of nanowires have values of t_{min} that scale closely with the wire diameter, D: $t_{min} \approx 2.33D$.[42] In fact eq 2 fits the high R_s/Z_0 data in Figure 1F very well, giving fit values of Π = 26 and n = 5.6 (again, these values have been used to plot eq 2 on Figure 1G for comparison). This value of Π is somewhat below the median value of 31.7 for metallic nanowire networks, probably due to the low value of $\sigma_{dc,B}/\sigma_{Op}$.[43] In addition, the percolation exponent is higher than typical values found for metallic nanowire networks,[43] suggesting the networks to be somewhat non-uniform.[14]

The data in Figure 1 show that the AgNW networks studied here both resemble and behave similarly to

networks previously described in a number of papers. Critically, the optical and electrical properties of thick networks behave as expected for bulk-like films, while thinner networks are described by percolation theory. In fact it is known that such percolative behavior is almost always found for nanostructured transparent conductors.[43] In addition, the technologically relevant regime around T_R = 90 almost always falls in the percolative regime, at least for solution-processed networks.[43] This is important, as it means that any comprehensive understanding of nanostructured heaters will have to incorporate percolation theory in some form.

Heating Behavior: Time Dependence. In order to assess the performance of these networks as transparent heaters, we drove a fixed current through the networks (interelectrode separation, l = 2 cm, electrode width, w = 2 cm), measuring the surface temperature as a function of time. This was carried out for a number of networks of different thicknesses (and so different transmittances and sheet resistances) using a range of current values. In all cases the data were perfectly reproducible with no irreversible temperature effects observed. Examples of the resultant temperature *versus* time data are shown in Figure 2A for a network with T_R = 61% for a number of different applied currents. In all cases the temperature increased monotonically with time before eventually saturating.

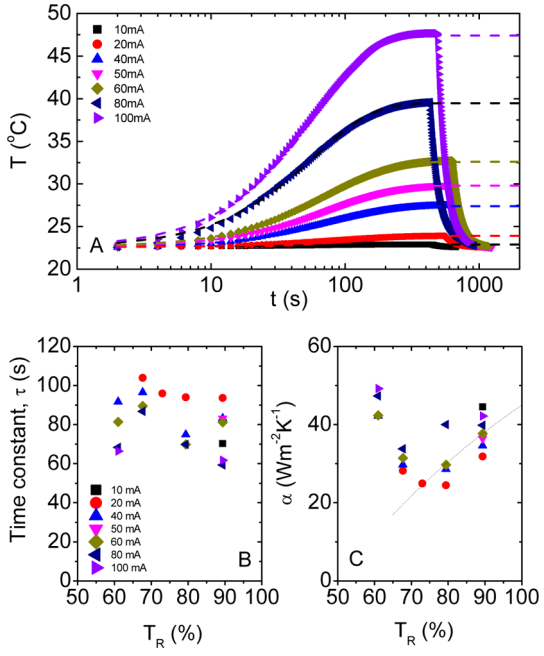

Figure 2. (A) Time dependence of temperature rise for an AgNW network (T_R = 61%) with a number of different applied currents. The dashed lines represent fits to eq 6. (B, C) Data derived from fitting time-dependent data such as that in A. (B) Time constant and (C) heat transfer constant, α, for AgNW networks as a function of network transmittance. In each case, data are shown for a range of applied currents. In C the dashed line represents the behavior suggested by eq 7b.

The saturation temperature depended on both the applied current and the network thickness (*i.e.*, transmittance).

To quantitatively analyze this data, it is necessary to develop a model that relates the time evolution of the temperature to the applied current and a parameter representing the network thickness, *e.g.*, the transmittance or the sheet resistance. We note that elements of such a model have been presented by Bae *et al.*[21] However, a full description such as that described here has not been reported. We can develop such a model by considering the energy balance between heating and dissipation. During current flow, the power dissipated by Joule heating in the AgNW network is given by $P_{in} = I^2R$, where R is the network resistance. Some of the dissipated power goes to increasing the temperature, T, of both the nanowire network and (*via* conduction) the substrate, while the remainder is lost *via* radiation and convection at both the nanowire network surface and the opposite surface of the substrate. Then, making the approximation that the instantaneous temperature is the same everywhere in both the network and the substrate, we can write a power balance equation:

$$I^2R = (m_1C_1 + m_2C_2)\frac{dT(t)}{dt} + A(h_1 + h_2)(T(t) - T_0) + \sigma A(\varepsilon_1 + \varepsilon_2)(T(t)^4 - T_0^4) \quad (4)$$

Here $T(t)$ and T_0 are the instantaneous sample temperature and the ambient temperature, A is the area of the film (assumed equal to the substrate area), and σ is the Stefan–Boltzmann constant. The subscripts 1 and 2 refer to the network and the substrate, respectively, such that m_1 and m_2 are the masses and C_1 and C_2 are the specific heat capacities of network and substrate. Similarly, h_1 and h_2 are the convective heat-transfer coefficients and ε_1 and ε_2 are the emissivities of the sides of the sample associated with the network and substrate, respectively. The term on the left of eq 4 is the dissipated electrical power, while the first term on the right describes the portion of that power used to raise the temperature of both network and substrate. The second term on the right is an approximate representation of the energy lost by convection, while the third term on the right represents the net energy lost radiatively (taking into account the thermal radiation absorbed from the environment).

Unfortunately no simple analytical solution exists for this differential equation. However, we can simplify it somewhat by noting that for small temperature rises (*i.e.*, $T(t) - T_0 < 40$ K) we can apply a Taylor expansion to give $T(t)^4 - T_0^4 \approx 4T_0^3(T(t) - T_0)$. This allows us to approximate the energy balance expression as

$$(m_1C_1 + m_2C_2)\frac{dT(t)}{dt} + A[(h_1 + h_2) + 4T_0^3\sigma(\varepsilon_1 + \varepsilon_2)](T(t) - T_0) - I^2R \approx 0 \quad (5)$$

This equation can be solved analytically to give

$$T(t) \approx T_0 + \frac{1}{\alpha}\frac{I^2R}{A}\left[1 - \exp\left(-\frac{\alpha}{C_2m_2/A}t\right)\right] \quad (6)$$

where I^2R/A is the areal power density. We note that the network is much less massive than the substrate, leading to the approximation $m_1C_1 \ll m_2C_2$. In addition, we introduce the symbol α for the quantity

$$\alpha = (h_1 + h_2) + 4(\varepsilon_1 + \varepsilon_2)\sigma T_0^3 \quad (7a)$$

where we refer to α as the heat transfer constant.

We have fitted eq 6 to the experimental data for $T(t)$. We found very good fits in all cases, as illustrated in Figure 2A. From the fits we can extract the time constant $\tau = m_2C_2/(A\alpha)$, which we plot *versus* network transmittance (*i.e.*, a measure of network thickness or density) in Figure 2B. While the data are somewhat scattered, all values cluster between 60 and 100 s, on the same order of magnitude as time constants reported by other researchers.[21,22,25−27,29,30,36,37]

From the fits, we can independently extract α. This is plotted *versus* the network transmittance in Figure 2C. This shows the heat transfer constant to lie in the range 25−50 W m^{-2} K^{-1} depending on the network thickness. While the emissivity of the AgNW network is not known, the emissivity of PET is known to be reasonably high; $\varepsilon_2 \approx 0.9$. This means the radiative contribution to α from the PET substrate side of the system is $\sim 4\varepsilon_2\sigma T_0^3 \approx 6$ W m^{-2} K^{-1}. Roughly extrapolating the experimental data to $T_R = 100\%$ suggests that for PET alone $\alpha \approx 40$ W m^{-2} K^{-1} (for both sides). Combining this with the radiative heat loss from PET implies that the convective heat-transfer coefficient of PET is $h_2 \approx 14$ W m^{-2} K^{-1}, close to that of glass ($h_{glass} \approx 10$ W m^{-2} K^{-1}).[21] Thus, depending on the network thickness, heat loss from the AgNW-coated surface contributes $\sim$5−30 W m^{-2} K^{-1} to the observed value of α (with the PET substrate side contributing $\sim$20 W m^{-2} K^{-1}). The maximum radiative contribution to α from the AgNW-coated surface is $4\sigma T_0^3 \approx 6$ (*i.e.*, if $\varepsilon_1 = 1$). This means that convective heat loss from the AgNW-coated surface is likely to dominate the heat loss process with values of $h_1 \approx 0$−24 W m^{-2} K^{-1} depending on the network thickness. This is consistent with values of $h = 8$−92 W m^{-2} K^{-1} previously observed for nanostructured or metallic films.[21] In addition, it confirms that both convection and radiation are significant heat loss pathways. This is different from graphene films, where heat loss is almost completely due to convection because of the low emissivity of graphene.[21]

We can begin to understand the dependence of α on transmittance by noting that heat convection and radiation are interfacial phenomena. On the network side of the sample, for very low nanowire coverage, the solid−air interface has contributions from both PET and AgNWs. Under these circumstances, h_1 and α_1 will depend on the convective heat-transfer coefficients and emissivities of both PET and nanowires as well as the area fraction of surface coated with nanowires, f_{NW}. At low coverage and so high transmittance, we can make the approximations that $h_1 = f_{NW}h_{NW} + (1 - f_{NW})h_{PET}$ and $\varepsilon_1 = f_{NW}\varepsilon_{NW} + (1 - f_{NW})\varepsilon_{PET}$, while of course $h_2 = h_{PET}$ and $\varepsilon_2 = \varepsilon_{PET}$. Using this approximation, eq 7a becomes

$$\alpha = 2(h_{PET} + 4\varepsilon_{PET}\sigma T_0^3) - f_{NW}[(h_{PET} - h_{NW}) + 4\sigma T_0^3(\varepsilon_{PET} - \varepsilon_{NW})] \quad (7b)$$

We assume for simplicity that we can relate the transmittance to the amount of nanowires coating the substrate using the Lambert−Beer law: $f_{NW} \propto -\log T_R$, allowing us to write $\alpha = K_1 + K_2 \log T_R$. This functional form has been plotted in Figure 2C and is consistent with the high T_R data as long as $K_2 > 0$.

While values of h_{NW} and ε_{NW} are not known, AgNW networks are known to exhibit thermal shielding behavior,[49] leading to low values of ε_{NW} compared to other materials, suggesting $\varepsilon_{PET} - \varepsilon_{NW}$ would be positive. Then, that $K_2 > 0$ implies that $h_{PET} - h_{NW} > 0$, at least at low coverage. However, the behavior described by eq 7b breaks down for $T_R < 80\%$ (Figure 2C). However, this is not surprising, as Figure 1E shows f_{NW} to be quite high at this transmittance, probably invalidating the assumptions leading to eq 7b for low T_R values.

As T_R falls below 80%, α begins to increase with decreasing T_R (*i.e.*, with increasing nanowire coverage). However, in this regime, h_{NW} is probably controlled by network properties such as surface roughness[50] and high internal surface area. This may result in an increase in h_{NW} with increasing coverage, leading to the observed behavior.

Heating Behavior: Steady State. The steady-state temperature, T_{Sat}, can be found from eq 5 by setting $dT/dt = 0$. This gives

$$T_{sat} = T_0 + \frac{I^2R}{\alpha A} = T_0 + \frac{I^2R_s}{\alpha w^2} \quad (8)$$

where we have used $R = R_sl/w$ and $A = lw$. To test this, we applied a range of currents to a number of networks of various thicknesses. We measured the steady-state temperature after $\sim$10 min, when it had clearly saturated. Shown in Figure 3A is a graph of the steady-state temperature increase, $\Delta T = T_{Sat} - T_0$, plotted *versus* the applied current for a number of different networks. It is clear from this data that $\Delta T \propto I^2$ for all networks studied. We have plotted the temperature rise *versus* the areal power density (*i.e.*, the power inputted by Joule heating per unit area) in Figure 3B. To a first approximation it is clear that all samples fall roughly on the same master curve such that $\Delta T \propto I^2R/A$. However,

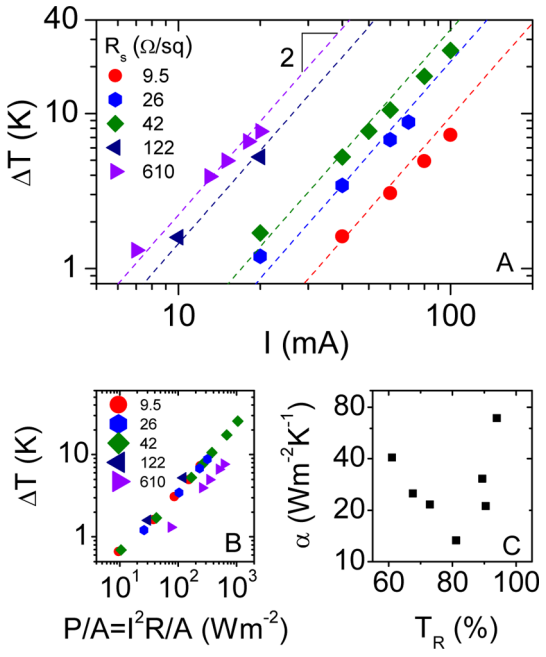

Figure 3. (A) Steady-state temperature, ΔT, rise plotted as a function of current, I, for networks with different sheet resistance, R_s (*i.e.*, different thicknesses and so transmittances). The dashed lines represent $\Delta T \propto I^2$. (B) Temperature rise plotted as a function of areal power density. The labels give the film sheet resistance. (C) Heat transfer constant, α, calculated from the slope of the curves in A and plotted *versus* film transmittance. In all cases the interelectrode separation l = 2 cm and the electrode width w = 2 cm. In A and B only some of the data sets are shown to avoid clutter.

a closer look shows some deviation from a single master curve. These deviations are consistent with variations in α from sample to sample. From the fit curves shown in Figure 3A we can calculate α using eq 8. We have plotted α *versus* the network transmittance, T_R, in Figure 3C. We find behavior very similar to that found by fitting the time-dependent data (Figure 2C). This shows that the model fits both time-dependent and steady-state data extremely well.

We note that eq 8 predicts ΔT to scale linearly with power (I^2R in our notation). Such behavior has been reported by a number of other authors for nanostructured transparent heaters.[21−24,26,28,29] This allows us to use eq 8 to analyze previously reported data to extract α. The results are given in the SI and show values of α in the range 15−123 W m^{-2} K^{-1}. Averaging the results by material gave mean values of 21 W m^{-2} K^{-1} (graphene), 70 W m^{-2} K^{-1} (nanotubes), and 39 W m^{-2} K^{-1} (metallic nanowires).

Relating Temperature to Transmittance. Once we know that the simple model outlined above describes the data reasonably well, we can extend it to describe the relationship between temperature increase and transmittance. To do this for bulk-like networks, we simply rearrange eq 1 for R_s and substitute into eq 8 to give

$$\frac{\Delta T}{I^2} = \frac{Z_0}{2\alpha w^2}\frac{\sigma_{Op}}{\sigma_{dc,B}}\left(\frac{1}{\sqrt{T_R}} - 1\right)^{-1} \quad (9)$$

We can apply the same procedure to describe networks in the percolative regime, except this time using eq 2 instead of eq 1:

$$\frac{\Delta T}{I^2} = \frac{1}{\Pi^{n+1}}\frac{Z_0}{\alpha w^2}\left(\frac{1}{\sqrt{T_R}} - 1\right)^{-(n+1)} \quad (10)$$

These equations imply that $\Delta T/I^2$ should scale with $T_R^{-1/2} - 1$ as a power law with an exponent that reflects whether the networks are in the bulk-like regime (*i.e.*, thicker networks give exponent = −1) or the percolative regime (*i.e.*, thinner networks give exponent = $-(n + 1)$). To test this, we plotted $\Delta T/I^2$ *versus* $T_R^{-1/2} - 1$ for all samples (*i.e.*, different thicknesses and currents) in Figure 4A on a log−log plot. We do indeed find two separate regions described by different power laws. To demonstrate consistency with our model, we plot the curves described by eqs 9 and 10 alongside the data in Figure 4A using the parameters given above (*i.e.*, w = 2 cm, $\sigma_{dc,B}/\sigma_{Op}$ =70, Π = 26, and n = 5.6). Because α is weakly thickness dependent, we use a representative value: α = 40 W m^{-2} K^{-1}. The resultant curves overlay the data extremely well.

Figure 4A clearly illustrates the fact that the relationship between temperature and transmittance in AgNW networks differs between percolative and bulk regimes. Because Joule heating increases with the electrical resistance of the network, it is not surprising that $\Delta T/I^2$ values are higher for the less dense, more transparent networks. Therefore, at first glance the percolative regime appears most suitable for applications. This apparent supremacy of more resistive networks seems to be reinforced by comparison with literature data for transparent heaters fabricated from SWNTs and AgNWs (Figure 4A). The AgNW data lie slightly below the data generated here, while data for the more resistive SWNT networks show significantly larger values of $\Delta T/I^2$. This implies SWNT networks give a larger temperature rise per unit current compared to AgNW networks. However, closer examination shows this to be very misleading: more resistive networks are not better transparent heaters. The reason is that more resistive networks require more power to drive a given current and so reach a given temperature increase. This makes them less efficient overall. We perform quantitative analysis to demonstrate this below.

Operating Voltage and Figures of Merit. The analysis above shows that the model we have described fits real data extremely well. This allows us to consider what properties are required of a network to work in a real transparent heater application. It is likely that the details of the application will set ΔT and T_R as well as the heater dimensions, *i.e.*, l and w. Then, ΔT will define the required power *via* eq 8, while T_R will define R_s *via* eq 1 or 2, depending on whether the network is bulk-like or percolative. Then the aim will be to achieve the required ΔT given the set value of T_R (and so R_s) for the lowest applied voltage, V. This will then minimize the

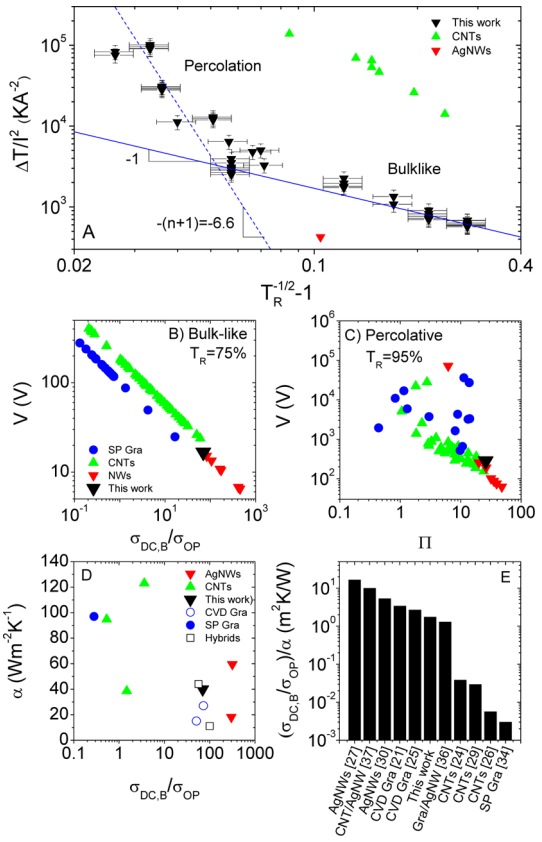

Figure 4. Temperature rise over current squared ($\Delta T/I^2$) plotted *versus* $T_R^{-1/2} - 1$ for all networks at all applied currents. Note the latter parameter is proportional to network thickness. Measurements at all currents have collapsed onto the same master curve. The lines are plots of eq 9 (solid) and eq 10 (dashed), representing behavior in the bulk-like and percolative regimes, respectively. Also shown are data extracted from the literature for SWNT networks[29] (green) and an AgNW network[22] (red). (B) Predicted voltage required to reach a steady-state temperature increase of 40 K as a function of $\sigma_{dc,B}/\sigma_{Op}$. The calculation assumes a bulk-like network with $T_R = 75\%$. The symbols represent reported values of $\sigma_{dc,B}/\sigma_{Op}$ for solution-processed graphene (SP Gra), carbon nanotube (CNTs), and AgNW networks.[43] (C) Plot of voltage required to reach a steady-state temperature increase of 40 K as a function of percolative figure of merit, Π. The symbols represent data points calculated using known values of Π and *n* for solution-processed graphene, nanotube, and AgNW networks.[43] The calculation assumes a percolative network with $T_R = 95\%$. Also included in B and C are values of *V* calculated for the networks studied in this work. In both B and C, the calculations use the following values: *l* = 10 cm, α/(W m^{-2} K^{-1}) = 21 (graphene), 70 (SWNTs), 39 (NWs), 40 (this work). (D) Comparison of performance of thermal heaters in the literature[21,24−27,29,30,34,36,37] with this work. Heat-transfer constant, α, plotted *versus* $\sigma_{dc,B}/\sigma_{Op}$, for a number of solution-processed (SP) graphene, CVD graphene, CNT, AgNW, and hybrid (*i.e.*, graphene AgNW and CNT/AgNW) transparent heaters. Both values were extracted by us from published data (see SI). (E) Thermal heater figure of merit, $(\sigma_{dc,B}/\sigma_{Op})/\alpha$, calculated from data in D. The bracketed number denotes the reference.

power because $P = I^2R = V^2/R$. Then, using eq 8 and changing the variable from current to voltage using $V = IR_s l/w$ gives an expression for the operating voltage:

$$V = \sqrt{\alpha \Delta T R_s I^2} \qquad (11)$$

where *l* represents the inter-electrode spacing. If, for example, the network is such that the required transmittance occurs in the bulk-like regime, then we can use eq 1 to replace R_s to give

$$V = \sqrt{\frac{\alpha \Delta T Z_0 I^2}{2(T_R^{-1/2} - 1)\sigma_{dc,B}/\sigma_{Op}}} \qquad (12)$$

where *l* represents the inter-electrode spacing. This expression clearly shows that to minimize *V*, we need a network material with a low α and high $\sigma_{dc,B}/\sigma_{Op}$. Because this equation describes the bulk-like regime, it is appropriate only for networks with relatively low transmittances. The transmittance where a network changes from bulk-like to percolative depends on the specific nanomaterial being used. However, De *et al.* have shown that most networks are bulk-like for T_R = 75%.[43] Thus, for descriptive purposes, we use eq 12 to find the voltage required to induce a temperature increase of 40 K in a network (T_R = 75%) fabricated from the wires described here to be *V* = 17 V (using *l* = 0.1 m, α = 40 W m^{-2} K^{-1}, and $\sigma_{dc,B}/\sigma_{Op}$ = 70).

For comparison purposes, we can calculate this operating voltage for transparent heaters fabricated from networks (T_R = 75%) of a number of different nanostructured transparent conductors that have been described in the literature. To do this, we use the values of α extracted from the literature as described above. In addition, we make use of a recent review that has tabulated values of $\sigma_{dc,B}/\sigma_{Op}$ for solution-processed networks of graphene, nanotubes and metallic nanowires.[43] We use these tabulated values of $\sigma_{dc,B}/\sigma_{Op}$ coupled with the values of α reported above to predict the voltage, *V*, required to achieve a steady-state temperature rise of 40 K for these previously reported networks of metallic nanowires, SWNTs, and graphene (all solution-processed and taking *l* = 10 cm, Figure 4B). The data in Figure 4B show that metallic nanowire networks require values of *V* < 16 V (median 10 V). However, solution-processed SWNT and graphene networks require voltages in the range 23−730 V (median 85 V) and 25−4500 V (median 172 V), respectively.

However, it is more likely[43] that the required transmittance will be considerably above 70% (usually $T_R \approx 85-95\%$) and so will occur in the percolative regime for solution-processed networks.[42] Then we can use eq 2 to replace R_s in eq 8 (and using $V = IR_s l/w$) to give

$$V = \sqrt{\frac{\alpha \Delta T Z_0 I^2}{[(T_R^{-1/2} - 1)\Pi]^{(n+1)}}} \qquad (13)$$

Applying this to our AgNW networks shows that *V* = 283 V is required to raise the temperature by 40 K for a percolative network that is 95% transparent (*l* = 10 cm, α = 25 W m^{-2} K^{-1}, Π = 26, *n* = 5.6). This value is very high, clearly showing the problems associated with very thin nanostructured networks. Using literature

data for Π and n tabulated by De *et al.*[43] and the values of α given above, we can calculate the voltage required for a 40 K rise for transparent heaters prepared from very thin networks of metallic nanowires, SWNTs, and graphene (T_R = 95%, l = 10 cm, Figure 4C). These are plotted as a function of Π in Figure 4C, which shows that metallic nanowire networks require values of V as low as 60 V. However, SWNT and graphene networks require voltages that are >300 and >500 V, respectively. These results show that for solution-processed networks metallic nanowires are far superior to networks of nanotubes or graphene.

However, it is also very important to note the effect of percolation on nanowire performance. In general, increasing the transmittance of a heater from 75% to 95% involves moving from a network that is bulk-like to one that is percolative. According to the data in Figure 4B,C, this will result in an order of magnitude increase in operating voltage for networks of metallic nanowires. This will result in massive efficiency reduction and is obviously prohibitive. It is clear that networks that can retain bulk-like behavior at low enough thickness such that $T_R \approx 90-95\%$ will be important for transparent heaters. Because the thickness (and so transmittance) defining the bulk to percolative transition depends on the diameter/thickness of the nanowires/nanosheets making up the network,[42] thinner nanostructures (*i.e.*, lower diameter nanowires/nanotubes or thinner nanosheets) will result in higher efficiency.

It is clear from eq 12 that, for bulk-like networks, the material parameters that control the performance of thermal heaters are α and $\sigma_{dc,B}/\sigma_{Op}$. For low operating voltages, low values of α coupled with high values of $\sigma_{dc,B}/\sigma_{Op}$ will be required. For percolative networks, the equivalent parameters would be α and Π^{n+1}. We note that with the exception of one paper[21] none of the published work on transparent heaters give values of α,$\sigma_{dc,B}/\sigma_{Op}$, n, or Π. In addition, none of these papers give enough information to ascertain whether they are bulk-like or percolative (there are two papers on CVD-grown graphene, which is clearly not a percolative material[21,25]). However, for simplicity we assume all are bulk-like, and, where possible, we extracted values of α and $\sigma_{dc,B}/\sigma_{Op}$ from the reported data (see the SI). We did this for three papers based on CNTs,[24,26,29] two papers based on CVD graphene,[21,25] one paper on solution-processed graphene (SP Gra),[34] two papers based on AgNW networks,[27,30] and two papers based on hybrid structures.[36,37] We plot α *versus* $\sigma_{dc,B}/\sigma_{Op}$ in Figure 4D, including the results from this paper for comparison. Given that small α and large $\sigma_{dc,B}/\sigma_{Op}$ are required for effective performance, it is clear that CVD graphene and AgNW networks are far superior to CNT or solution-processed graphene transparent heaters.

We can see this in another way by noting that inspection of eq 12 shows that $(\sigma_{dc,B}/\sigma_{Op})/\alpha$ can be used as a figure of merit for bulk-like transparent heaters (higher values give better performance). We have used the data in Figure 4D to plot a bar chart of $(\sigma_{dc,B}/\sigma_{Op})/\alpha$ in Figure 4E. This clearly shows that AgNW networks appear to have the most promise, followed closely by CVD graphene, with CNT networks falling far behind. Similar considerations would suggest Π^{n+1}/α as a figure of merit for percolative transparent heaters. Because of the relationship between Π and $\sigma_{dc,B}/\sigma_{Op}$ (eq 3), we expect the materials ranking for percolative networks to be the same as for bulk-like networks.

CONCLUSION

In conclusion, we have prepared transparent conductors from networks of silver nanowires and shown them to work effectively as transparent heaters. By considering the balance of Joule heating and energy dissipation by both radiation and convection, we have developed a comprehensive model relating the heater temperature as a function of time to electrical and thermal parameters. This model described the temperature very well in both time-dependent and steady-state regimes.

Like most nanostructured systems, these AgNW networks have electrical properties that are bulk-like for thick networks but percolative for thin networks. By combining the model described above with equations relating optical transmittance to network sheet resistance in both bulk-like and percolative regimes, it is possible to generate expressions relating the steady-state temperature to transmittance and current. These expressions predict significantly different heating behavior in the bulk-like and percolative regimes. This prediction is borne out by the data with theory and experiment matching extremely well.

A good transparent heater is one that achieves a given temperature rise at as low a voltage as possible. With this in mind, the models described above can be used to suggest figures of merit for both bulk-like and percolative networks: $(\sigma_{dc,B}/\sigma_{Op})/\alpha$ and Π^{n+1}/α, respectively. High values of these parameters will lead to low operating voltages. This work suggests AgNW networks to be most promising, followed by CVD graphene, followed by solution-processed nanotube and graphene networks. This ranking should apply in both bulk-like and percolative regimes.

This work provides the first comprehensive, integrated description of the physics of nanostructured transparent heaters. It clearly demonstrates the parameters that are important for effective and efficient heater operation and allows the identification of

materials that can fulfill the resultant criteria. We believe this information will be very useful to the development of nanostructured transparent heaters for real applications.

METHODS

For this study, silver nanowires (AgNWs) were synthesized by Kechuang (http://www.ke-chuang.com/) and supplied as a suspension in isopropyl alcohol (IPA) (C_{AgNW} = 16 mg mL^{-1}). These nanowires had a mean length of ~5 μm and mean diameter of ~50 nm. A small volume of the dispersion was diluted to 1.5 mg mL^{-1} in IPA and subjected to 30 s low power sonication in a sonic bath (Model Ney Ultrasonic) to eliminate bundles of nanowires. This solution was then further diluted to 0.15 mg mL^{-1} and sonicated another 30 s immediately before being sprayed[14] onto PET squares of 2 × 2 cm and thickness 135 μm on a hot plate at 120 °C. The temperature was kept high during spraying in order to evaporate the IPA swiftly and remove polymer residue left over from synthesis.

Optical transmission spectra were recorded using a Cary Varian 6000i, with a sheet of PET used as the reference. Sheet resistance measurements were made using the four-probe technique using a Keithley 2400 source meter. Scanning electron microscopy and helium ion microscopy images were taken using a Zeiss Ultra scanning electron microscope and Carl Zeiss Orion PLUS Helium Ion microscope, respectively.

For temperature measurements, AgNW films on PET were used. To measure the temperature, a low mass thermistor was used. This was housed inside a hole in the side of a U-shaped copper clamp (secured using nail polish) and was held in place at the midpoint between the silver electrodes (at the edge of the sample) using a small screw. Electrical measurements were made using a Keithley source meter. For a given measurement, at time $t = 0$, a predefined current was driven through the AgNW film, resulting in an increase in the film temperature and so a change in thermistor resistance. The change in resistance was recorded using MATLAB, and the temperature was extracted using the thermistor's calibration curve. The temperature was recorded as a function of time over the course of 15 min, significantly longer that the necessary time for the temperature to reach steady-state. Stabilizing the experimental environment was vital since the lab temperature could fluctuate by up to 3 °C. The system was sheltered from the ambient lab using a copper bell jar covered with commercially available insulating foam.

Conflict of Interest: The authors declare no competing financial interest.

Supporting Information Available: Analysis of literature data for nanostructured transparent heaters. This material is available free of charge *via* the Internet at http://pubs.acs.org.

Acknowledgment. We acknowledge the Science Foundation Ireland-funded collaboration (SFI grant 03/CE3/M406s1) between Trinity College Dublin and Hewlett-Packard, which has allowed this work to take place. We also acknowledge the Agence Nationale de la Recherche through the program Mat&pro and the project Fichtre. We thank Alan Bell and the CRANN Advanced Microscopy Lab for help with He ion microscopy.

REFERENCES AND NOTES

1. Ellmer, K. Past Achievements and Future Challenges in the Development of Optically Transparent Electrodes. *Nat. Photonics* **2012**, *6*, 808–816.
2. Gordon, R. G. Criteria for Choosing Transparent Conductors. *MRS Bull.* **2000**, *25*, 52–57.
3. Chen, Z.; Cotterell, B.; Wang, W. The Fracture of Brittle Thin Films on Compliant Substrates in Flexible Displays. *Eng. Fract. Mech.* **2002**, *69*, 597–603.
4. Hu, L.; Hecht, D. S.; Gruner, G. Percolation in Transparent and Conducting Carbon Nanotube Networks. *Nano Lett.* **2004**, *4*, 2513–2517.
5. Wu, Z. C.; Chen, Z. H.; Du, X.; Logan, J. M.; Sippel, J.; Nikolou, M.; Kamaras, K.; Reynolds, J. R.; Tanner, D. B.; Hebard, A. F.; *et al*. Transparent, Conductive Carbon Nanotube Films. *Science* **2004**, *305*, 1273–1276.
6. Hecht, D. S.; Heintz, A. M.; Lee, R.; Hu, L. B.; Moore, B.; Cucksey, C.; Risser, S. High Conductivity Transparent Carbon Nanotube Films Deposited from Superacid. *Nanotechnology* **2011**, *22*, 075201.
7. De, S.; Coleman, J. N. Are There Fundamental Limitations on the Sheet Resistance and Transmittance of Thin Graphene Films? *ACS Nano* **2010**, *4*, 2713–2720.
8. Wang, X.; Zhi, L.; Mullen, K. Transparent, Conductive Graphene Electrodes for Dye-Sensitized Solar Cells. *Nano Lett.* **2007**, *8*, 323–327.
9. De, S.; Higgins, T.; Lyons, P. E.; Doherty, E. M.; Nirmalraj, P. N.; Blau, W. J.; Boland, J. J.; Coleman, J. N. Silver Nanowire Networks as Flexible, Transparent, Conducting Films: Extremely High dc to Optical Conductivity Ratios. *ACS Nano* **2009**, *3*, 1767–1774.
10. Hu, L. B.; Kim, H. S.; Lee, J. Y.; Peumans, P.; Cui, Y. Scalable Coating and Properties of Transparent, Flexible, Silver Nanowire Electrodes. *ACS Nano* **2010**, *4*, 2955–2963.
11. Lee, J. Y.; Connor, S. T.; Cui, Y.; Peumans, P. Solution-Processed Metal Nanowire Mesh Transparent Electrodes. *Nano Lett.* **2008**, *8*, 689–692.
12. Madaria, A. R.; Kumar, A.; Ishikawa, F. N.; Zhou, C. W. Uniform, Highly Conductive, and Patterned Transparent Films of a Percolating Silver Nanowire Network on Rigid and Flexible Substrates Using a Dry Transfer Technique. *Nano Res.* **2010**, *3*, 564–573.
13. Madaria, A. R.; Kumar, A.; Zhou, C. W. Large Scale, Highly Conductive and Patterned Transparent Films of Silver Nanowires on Arbitrary Substrates and Their Application in Touch Screens. *Nanotechnology* **2011**, *22*, 245201.
14. Scardaci, V.; Coull, R.; Lyons, P. E.; Rickard, D.; Coleman, J. N. Spray Deposition of Highly Transparent, Low-Resistance Networks of Silver Nanowires over Large Areas. *Small* **2011**, *7*, 2621–2628.
15. Wu, H.; Hu, L. B.; Rowell, M. W.; Kong, D. S.; Cha, J. J.; McDonough, J. R.; Zhu, J.; Yang, Y. A.; McGehee, M. D.; Cui, Y. Electrospun Metal Nanofiber Webs as High-Performance Transparent Electrode. *Nano Lett.* **2010**, *10*, 4242–4248.
16. Lyons, P. E.; De, S.; Elias, J.; Schamel, M.; Philippe, L.; Bellew, A. T.; Boland, J. J.; Coleman, J. N. High-Performance Transparent Conductors from Networks of Gold Nanowires. *J. Phys. Chem. Lett.* **2011**, *2*, 3058–3062.
17. Rathmell, A. R.; Wiley, B. J. The Synthesis and Coating of Long, Thin Copper Nanowires to Make Flexible, Transparent Conducting Films on Plastic Substrates. *Adv. Mater. (Weinheim, Ger.)* **2011**, *23*, 4798–4803.
18. Bae, S.; Kim, H.; Lee, Y.; Xu, X. F.; Park, J. S.; Zheng, Y.; Balakrishnan, J.; Lei, T.; Kim, H. R.; Song, Y. I.; *et al*. Roll-to-Roll Production of 30-Inch Graphene Films for Transparent Electrodes. *Nat. Nanotechnol.* **2010**, *5*, 574–578.
19. King, P. J.; Higgins, T. M.; De, S.; Nicoloso, N.; Coleman, J. N. Percolation Effects in Supercapacitors with Thin, Transparent Carbon Nanotube Electrodes. *ACS Nano* **2012**, *6*, 1732–1741.
20. Sorel, S.; Khan, U.; Coleman, J. N. Flexible, Transparent Dielectric Capacitors with Nanostructured Electrodes. *Appl. Phys. Lett.* **2012**, *101*, 103106.
21. Bae, J. J.; Lim, S. C.; Han, G. H.; Jo, Y. W.; Doung, D. L.; Kim, E. S.; Chae, S. J.; Huy, T. Q.; Luan, N. V.; Lee, Y. H. Heat Dissipation of Transparent Graphene Defoggers. *Adv. Funct. Mater.* **2012**, *22*, 4819–4826.
22. Celle, C.; Mayousse, C.; Moreau, E.; Basti, H.; Carella, A.; Simonato, J. P. Highly Flexible Transparent Film Heaters Based on Random Networks of Silver Nanowires. *Nano Res.* **2012**, *5*, 427–433.

23. Janas, D.; Koziol, K. K. Rapid Electrothermal Response of High-Temperature Carbon Nanotube Film Heaters. *Carbon* **2013**, *59*, 457–463.
24. Jang, H. S.; Jeon, S. K.; Nahm, S. H. The Manufacture of a Transparent Film Heater by Spinning Multi-Walled Carbon Nanotubes. *Carbon* **2011**, *49*, 111–116.
25. Kang, J.; Kim, H.; Kim, K. S.; Lee, S. K.; Bae, S.; Ahn, J. H.; Kim, Y. J.; Choi, J. B.; Hong, B. H. High-Performance Graphene-Based Transparent Flexible Heaters. *Nano Lett.* **2011**, *11*, 5154–5158.
26. Kang, T. J.; Kim, T.; Seo, S. M.; Park, Y. J.; Kim, Y. H. Thickness-Dependent Thermal Resistance of a Transparent Glass Heater with a Single-Walled Carbon Nanotube Coating. *Carbon* **2011**, *49*, 1087–1093.
27. Kim, T.; Kim, Y. W.; Lee, H. S.; Kim, H.; Yang, W. S.; Suh, K. S. Uniformly Interconnected Silver-Nanowire Networks for Transparent Film Heaters. *Adv. Funct. Mater.* **2013**, *23*, 1250–1255.
28. Wu, Z. P.; Wang, J. N. Preparation of Large-Area Double-Walled Carbon Nanotube Films and Application as Film Heater. *Physica E* **2009**, *42*, 77–81.
29. Yoon, Y. H.; Song, J. W.; Kim, D.; Kim, J.; Park, J. K.; Oh, S. K.; Han, C. S. Transparent Film Heater Using Single-Walled Carbon Nanotubes. *Adv. Mater. (Weinheim, Ger.)* **2007**, *19*, 4284–4287.
30. Wang, S. H.; Zhang, X.; Zhao, W. W. Flexible, Transparent, and Conductive Film Based on Random Networks of Ag Nanowires. *J. Nanomater.* **2013**, *2013*, 456098.
31. http://www.minco.com/~/media/WWW/Resource%20-Library/Heaters/Whitepapers/Minco_HTCThinfilm.ashx.
32. http://www.imatproject.eu/.
33. Mcmaster, H. A. Conductive Coating for Glass and Method of Application. U.S. patent US2429420 A, 1947.
34. Sui, D.; Huang, Y.; Huang, L.; Liang, J. J.; Ma, Y. F.; Chen, Y. S. Flexible and Transparent Electrothermal Film Heaters Based on Graphene Materials. *Small* **2011**, *7*, 3186–3192.
35. Langley, D.; Giusti, G.; Mayousse, C.; Celle, C.; Bellet, D.; Simonato, J. P. Flexible Transparent Conductive Materials Based on Silver Nanowire Networks: A Review. *Nanotechnology* **2013**, *24*, 452001.
36. Zhang, X.; Yan, X.; Chen, J.; Zhao, J. Large-Size Graphene Microsheets as a Protective Layer for Transparent Conductive Silver Nanowire Film Heaters. *Carbon* **2014**, *69*, 437–443.
37. Kim, D.; Zhu, L. J.; Jeong, D. J.; Chun, K.; Bang, Y. Y.; Kim, S. R.; Kim, J. H.; Oh, S. K. Transparent Flexible Heater Based on Hybrid of Carbon Nanotubes and Silver Nanowires. *Carbon* **2013**, *63*, 530–536.
38. Leem, D.-S.; Edwards, A.; Faist, M.; Nelson, J.; Bradley, D. D. C.; de Mello, J. C. Efficient Organic Solar Cells with Solution-Processed Silver Nanowire Electrodes. *Adv. Mater. (Weinheim, Ger.)* **2011**, *23*, 4371–4375.
39. Liu, C.-H.; Yu, X. Silver Nanowire-Based Transparent, Flexible, and Conductive Thin Film. *Nanoscale Res. Lett.* **2011**, *6*, 75.
40. Sorel, S.; Lyons, P. E.; De, S.; Dickerson, J. C.; Coleman, J. N. The Dependence of the Optoelectrical Properties of Silver Nanowire Networks on Nanowire Length and Diameter. *Nanotechnology* **2012**, *23*, 185201.
41. van de Groep, J. V.; Spinelli, P.; Polman, A. Transparent Conducting Silver Nanowire Networks. *Nano Lett.* **2012**, *12*, 3138–3144.
42. De, S.; King, P. J.; Lyons, P. E.; Khan, U.; Coleman, J. N. Size Effects and the Problem with Percolation in Nanostructured Transparent Conductors. *ACS Nano* **2010**, *4*, 7064–7072.
43. De, S.; Coleman, J. N. The Effects of Percolation in Nanostructured Transparent Conductors. *MRS Bull.* **2011**, *36*, 774–781.
44. Dressel, M.; Grèuner, G. *Electrodynamics of Solids: Optical Properties of Electrons in Matter*; Cambridge University Press: Cambridge, 2002; p xii.
45. Barnes, T. M.; Reese, M. O.; Bergeson, J. D.; Larsen, B. A.; Blackburn, J. L.; Beard, M. C.; Bult, J.; van de Lagemaat, J. Comparing the Fundamental Physics and Device Performance of Transparent, Conductive Nanostructured Networks with Conventional Transparent Conducting Oxides. *Adv. Energy Mater.* **2012**, *2*, 353–360.
46. Doherty, E. M.; De, S.; Lyons, P. E.; Shmeliov, A.; Nirmalraj, P. N.; Scardaci, V.; Joimel, J.; Blau, W. J.; Boland, J. J.; Coleman, J. N. The Spatial Uniformity and Electromechanical Stability of Transparent, Conductive Films of Single Walled Nanotubes. *Carbon* **2009**, *47*, 2466–2473.
47. De, S.; Lyons, P. E.; Sorrel, S.; Doherty, E. M.; King, P. J.; Blau, W. J.; Nirmalraj, P. N.; Boland, J. J.; Scardaci, V.; Joimel, J.; *et al.* Transparent, Flexible, and Highly Conductive Thin Films Based on Polymer-Nanotube Composites. *ACS Nano* **2009**, *3*, 714–720.
48. King, P. J.; Khan, U.; Lotya, M.; De, S.; Coleman, J. N. Improvement of Transparent Conducting Nanotube Films by Addition of Small Quantities of Graphene. *ACS Nano* **2010**, *4*, 4238–4246.
49. Larciprete, M. C.; Albertoni, A.; Belardini, A.; Leahu, G.; Voti, R. L.; Mura, F.; Sibilia, C.; Nefedov, I.; Anoshkin, I. V.; Kauppinen, E. I.; *et al.* Infrared Properties of Randomly Oriented Silver Nanowires. *J. Appl. Phys.* **2012**, *112*, 083503.
50. Smith, J. W.; Epstein, N. Effect of Wall Roughness on Convective Heat Transfer in Commercial Pipes. *AIChE J.* **1957**, *3*, 242–248.